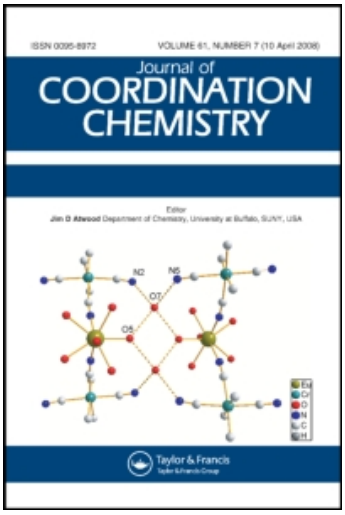

Journal of Coordination Chemistry
Publication details, including instructions for authors and subscription information:
http://www.informaworld.com/smpp/title~content=t713455674

A new layered vanadate complex with a tunnel structure: $[\{Cu(mbpy)\}_2V_8O_{21}]$ (mbpy = 4,4'-dimethyl-2,2'-bipyridine)

Zhangang Han[a]; Jingjing Wu[a]; Tao Chai[a]; Xueliang Zhai[a]
[a] College of Chemistry and Material Science, Hebei Normal University, Shijiazhuang, Hebei 050016, China

First published on: 11 June 2010

To cite this Article Han, Zhangang , Wu, Jingjing , Chai, Tao and Zhai, Xueliang(2010) 'A new layered vanadate complex with a tunnel structure: $[\{Cu(mbpy)\}_2V_8O_{21}]$ (mbpy = 4,4'-dimethyl-2,2'-bipyridine)', Journal of Coordination Chemistry, 63: 10, 1690 — 1699, First published on: 11 June 2010 (iFirst)
To link to this Article: DOI: 10.1080/00958972.2010.490295
URL: http://dx.doi.org/10.1080/00958972.2010.490295

Journal of Coordination Chemistry
Vol. 63, No. 10, 20 May 2010, 1690–1699

Taylor & Francis
Taylor & Francis Group

A new layered vanadate complex with a tunnel structure: $[\{Cu(mbpy)\}_2V_8O_{21}]$ (mbpy = 4,4′-dimethyl-2,2′-bipyridine)

ZHANGANG HAN*, JINGJING WU, TAO CHAI and XUELIANG ZHAI*

College of Chemistry and Material Science, Hebei Normal University,
Yuhua East Road 113, Shijiazhuang, Hebei 050016, China

(*Received 25 December 2009; in final form 25 February 2010*)

A new vanadate with a tunnel structure $[\{Cu(mbpy)\}_2V_8O_{21}]$ (**1**) (mbpy = 4,4′-dimethyl-2,2′-bipyridine) has been synthesized hydrothermally. X-ray crystal analysis reveals that **1** exhibits a layered structure constructed from $\{V_8O_{21}\}_n$ layers grafted with secondary metal coordination groups of Cu-mbpy. The thermogravimetric analysis and electrochemistry of **1** are also reported.

Keywords: Polyoxometalate; Vanadate; Layered structure; Hybrid; Copper

1. Introduction

Polyoxometalates (POMs) attract considerable interest because of their controllable shape and size, their highly negative charges, and their oxo-enriched surfaces [1–4]. A series of inorganic–organic hybrid polyvanadates have been reported due to their molecular and structural diversity and their significant applicability in a range of fields [5–8]. In ongoing efforts to develop synthetic and functional analogues of POM-based hybrids, secondary metal coordination groups (SMGs) have been widely used to assemble POM clusters into high-dimensional framework structures [9–12]. In these compounds, the SMGs not only provide charge compensation and become a part of the inorganic POM framework, but also enrich the frameworks of POMs and ameliorate their electronic and magnetic properties.

Layered vanadates are of particular interest owing to their intriguing variety of architectures [13–15] and their potential applications in reversible lithium ion batteries and heterogeneous catalysis [16, 17]. In this article, a new layered structure of vanadate, formulated as $[\{(Cu(mbpy)\}_2V_8O_{21}]$ (**1**) (mbpy = 4,4′-dimethyl-2,2′-bipyridine), has been isolated and characterized. Compound **1** represents a 2-D vanadium oxide layer based on alternate arrangement of $\{VO_5\}$ square pyramids and $\{VO_4\}$ tetrahedra.

*Corresponding authors. Email: hanzg116@yahoo.com.cn; xlzhai253@mail.hebtu.edu.cn

Journal of Coordination Chemistry
ISSN 0095-8972 print/ISSN 1029-0389 online
DOI: 10.1080/00958972.2010.490295

2. Experimental

2.1. *Synthesis and characterization*

In a typical synthesis for **1**, a mixture of V_2O_5 (130.0 mg), $CuSO_4 \cdot 5H_2O$ (180.0 mg), mbpy (35.0 mg), and H_2O (10.0 mL) was sealed in a 23 mL Teflon-lined stainless steel autoclave and heated for 5 days at 170°C. After cooling to room temperature, black crystals of **1** were isolated as a major phase. The pH of the system was kept at ~6.0 before and after the synthesis. Yield: 47% (based on V). Elemental Anal. (%): C 23.26, H 1.95, N 4.52, Cu 10.26, and V 32.89. Found (%): C 23.40, H 1.98, N 4.59, Cu 10.33, and V 32.72.

All reagents for syntheses were purchased from commercial sources and used as received. Elemental analyses (C, H, and N) were performed on a Perkin Elmer 2400 CHN elemental analyzer. Analysis for Cu and V were performed by inductively coupled plasma atomic emission spectroscopy (ICP–AES) using a POMES TJA inductively coupled plasma mass spectroscopy/spectrometer (ICP–MS). Infrared (IR) spectra were recorded in KBr pellets with a FT-IR 8900 IR spectrometer from 400 to 4000 cm^{-1}. Thermogravimetric analysis (TGA) was carried out using a Perkin Elmer TGA7 instrument in flowing N_2 with a heating rate of 10°C min^{-1}. Powder X-ray diffraction (XRD) was determined by a Bruker AXS D8 Advance diffractometer. Cyclic voltammograms (CV) were recorded on a 384B polarographic analyzer. A CHI 660 Electrochemical Workstation connected to a Digital-586 personal computer was used for the control of electrochemical measurements and for data collection. A conventional three-electrode system was used. The working electrode was a modified constant phase element (CPE). A Ag/AgCl (saturated KCl) electrode was used as a reference electrode and Pt gauze as a counter electrode. All potentials were measured and reported *versus* the Ag/AgCl electrode.

2.2. *Single-crystal XRD*

The data of **1** were collected with the approximate dimensions $0.19 \times 0.17 \times 0.15\,mm^3$ on a SMART APEX II CCD area detector diffractometer at 298(2) K using graphite-monochromated Mo-Kα radiation ($\lambda = 0.71073$ Å) and θ scans technique (2.00–25.01 was collected). Empirical absorption correction was applied. A total of 10,535 reflections were measured and the independent reflections were 3200 [$R_{(int)} = 0.0354$]. The structure was solved by direct methods using SHELXS-97 [18] and refined by full-matrix least-squares on F^2 using the SHELXL-97 program package. All non-hydrogen atoms were refined anisotropically. The hydrogens were fixed in ideal positions. All the crystal data and structure refinement details for **1** are given in table 1. Selected bond lengths are listed in table 2.

2.3. *Preparation of 1-CPE*

A total of 0.50 g graphite powder and 0.05 g **1** were mixed and ground together by agate mortar and pestle to achieve an even, dry mixture; 0.50 mL paraffin oil was added to this mixture and stirred with a glass rod; then the mixture was used to pack into a 3 mm inner diameter glass tube, and the surface was pressed tightly onto weighing paper with

Table 1. Crystal data and structure refinement for **1**.

Empirical formula	$C_{24}H_{24}Cu_2N_4O_{21}V_8$
Formula weight	1239.07
Temperature (K)	296(2)
Wavelength (Å)	0.71073
Crystal system	Triclinic
Space group	$P\bar{1}$
Unit cell dimensions (Å, °)	
a	8.9178(13)
b	10.4394(16)
c	11.3321(17)
α	68.173(2)
β	71.994(2)
γ	76.598(2)
Volume (Å^3), Z	923.2(2), 1
Calculated density (mg m^{-3})	2.229
Absorption coefficient (mm^{-1})	3.143
F(000)	606
Crystal size (mm^3)	$0.19 \times 0.17 \times 0.15$
θ range for data collection (°)	2.00–25.01
Limiting indices	$-10 \le h \le 10$; $-12 \le k \le 12$; $-13 \le l \le 13$
Reflections collected	10,535
Independent reflection	3200 [$R_{(int)} = 0.0354$]
Completeness to $\theta = 25.01$ (%)	97.8
Absorption correction	Empirical
Max. and min. transmission	0.6500 and 0.5866
Refinement method	Full-matrix least-squares on F^2
Data/restraints/parameters	3200/0/270
Goodness-of-fit on F^2	1.051
Final R indices [$I > 2\sigma(I)$]	$R_1 = 0.0422$, $wR_2 = 0.1043$
R indices (all data)	$R_1 = 0.0542$, $wR_2 = 0.1188$
Largest difference peak and hole (e Å^{-3})	0.957 and −0.739

Table 2. Selected bond lengths (Å) and angles (°) for **1**.

V(1)–O(7)	1.649(4)	V(3)–O(3)	1.686(4)
V(1)–O(4)	1.650(4)	V(3)–O(6)$^{\#2}$	1.801(4)
V(1)–O(6)	1.734(4)	V(4)–O(1)	1.615(4)
V(1)–O(5)	1.770(4)	V(4)–O(10)	1.693(4)
V(2)–O(8)	1.587(4)	V(4)–O(2)	1.7631(8)
V(2)–O(3)$^{\#1}$	1.940(4)	V(4)–O(5)$^{\#3}$	1.779(4)
V(2)–O(9)	1.945(4)	Cu(1)–O(11)	1.924(4)
V(2)–O(10)	1.947(4)	Cu(1)–O(4)	1.932(4)
V(2)–O(7)	1.979(4)	Cu(1)–N(1)	1.970(4)
V(3)–O(11)	1.653(4)	Cu(1)–N(2)	1.984(4)
V(3)–O(9)	1.675(4)	Cu(1)–O(1)	2.393(4)
O(7)–V(1)–O(4)	110.2(2)	O(3)$^{\#1}$–V(2)–O(7)	154.78(18)
O(7)–V(1)–O(6)	108.6(2)	O(9)–V(2)–O(7)	87.70(17)
O(4)–V(1)–O(6)	111.9(2)	O(10)–V(2)–O(7)	84.08(16)
O(7)–V(1)–O(5)	109.8(2)	O(11)–Cu(1)–O(4)	89.74(17)
O(4)–V(1)–O(5)	108.0(2)	O(11)–Cu(1)–N(1)	92.77(17)
O(6)–V(1)–O(5)	108.4(2)	O(4)–Cu(1)–N(1)	168.68(18)
O(8)–V(2)–O(3)$^{\#1}$	103.9(2)	O(11)–Cu(1)–N(2)	166.49(18)
O(8)–V(2)–O(9)	106.7(2)	O(4)–Cu(1)–N(2)	94.25(17)
O(3)$^{\#1}$–V(2)–O(9)	85.61(16)	N(1)–Cu(1)–N(2)	80.92(17)
O(8–V(2)–O(10)	105.57(19)	O(11)–Cu(1)–O(1)	96.54(17)
O(3)$^{\#1}$–V(2)–O(10)	88.68(17)	O(4)–Cu(1)–O(1)	92.45(17)
O(9)–V(2)–O(10)	147.69(18)	N(1)–Cu(1)–O(1)	98.22(16)
O(8)–V(2)–O(7)	101.3(2)	N(2)–Cu(1)–O(1)	96.18(17)

Symmetry transformations used to generate equivalent atoms: $^{\#1} -x, -y+1, -z+2$; $^{\#2} -x+1, -y+1, -z+2$; $^{\#3} -x+1, -y, -z+2$.

a copper rod through the back. Electrical contact was established with a copper rod through the back of the electrode.

3. Results and discussions

3.1. *Synthesis*

Generally, many factors affect the hydrothermal reactions, such as starting materials, pH, reaction temperature, reaction time, etc., In POM chemistry, the pH of the solution is very important in the isolation of phases of a given composition and structure. For polyoxovanadates, it is easier to form cage-like $\{V_{18}\}$, $\{V_{16}\}$, $\{V_{15}\}$, or $\{V_{14}\}$ shells encapsulating a guest X ($X = Cl^-$, Br^-, H_2O, etc.) at its center, in which the guest plays a template role in directing the assembly. It should be noted that this kind of cage-like cluster can be achieved in pH = 2–12 [19]. Comparing **1** with several compounds containing $[V_{16}O_{38}(Cl)]^{n-}$ [20], it can be found that the reaction time and the starting reactants ($CuSO_4$ instead of $CuCl_2$) may play key roles in constructing the 2-D vanadium-oxide network.

3.2. *Description of structure*

The single-crystal XRD analysis reveals that **1** consists of a 2-D vanadium-oxide network grafted with $[Cu(mbpy)]^{2+}$ groups. As shown in figure 1, the vanadium-oxide network in **1** consists of four crystallographically independent V centers, V(1), V(2), V(3), and V(4), with two kinds of coordination environments, tetrahedral for V(1), V(3), V(4), and square pyramidal for V(2). The secondary metal Cu(II) is five-coordinate with square-pyramidal geometry. The square base is constructed from two nitrogens from one mbpy, and two oxygens shared with $\{VO_4\}$ tetrahedra (Cu–O: 1.924(4), 1.932(4) and Cu–N: 1.970(4), 1.984(4) Å); the apex is occupied by O(1) with Cu(1)–O(1) distance of 2.393(4) Å. In **1**, except for O(8), all oxygens are μ_2-coordinated, bonded to two metal sites. The terminal O(8) is only coordinated to V(2) with a bond distance of 1.587(4) Å which is a typical V=O double bond. The four residual vertices located at the square base of $\{V(2)O_5\}$ polyhedron come from four μ_2-O atoms shared with V(1), V(4), and two V(3)′s with bond lengths V(2)–O(7) = 1.979(4), V(2)–O(9) = 1.945(4), V(2)–O(10) = 1.947(4), and V(2)–O(3ii) = 1.940(4) Å, respectively. The four-coordinate V(1), V(3), and V(4) share their four μ_2-O with adjacent $\{VO_4\}$, $\{VO_5\}$, and $\{CuN_2O_3\}$ polyhedra. These V–O bond lengths vary from 1.615(4) to 1.801(4) Å, the O–V–O angles are in the range of 107.3(2)–113.80(16)°, showing the distorted tetrahedral geometry of $\{VO_4\}$.

A structural feature of **1** is that all Cu/V polyhedra are only linked *via* corner-sharing mode. As shown in figure 2, these distorted $\{VO_5\}$ square pyramids and $\{VO_4\}$ tetrahedra connect alternatively with each other *via* corner-sharing to form an infinite $\{V_8O_{21}\}_n$ layer. In the V–O layer, $\{VO_4\}$ units fuse as distorted chains bridged by $\{VO_5\}$ units to form four-, five-, and six-membered rings. Therefore, the $\{V_8O_{21}\}_n$ layer may be viewed as an extended 2-D structure with a 4,5,6-net. Each $\{CuN_2O_5\}$ square pyramid attaches to three $\{VO_4\}$ tetrahedra of the vanadate-oxygen layer *via* corner-sharing. In addition, the framework of **1** can also be viewed as a 2-D net with tunnel structure

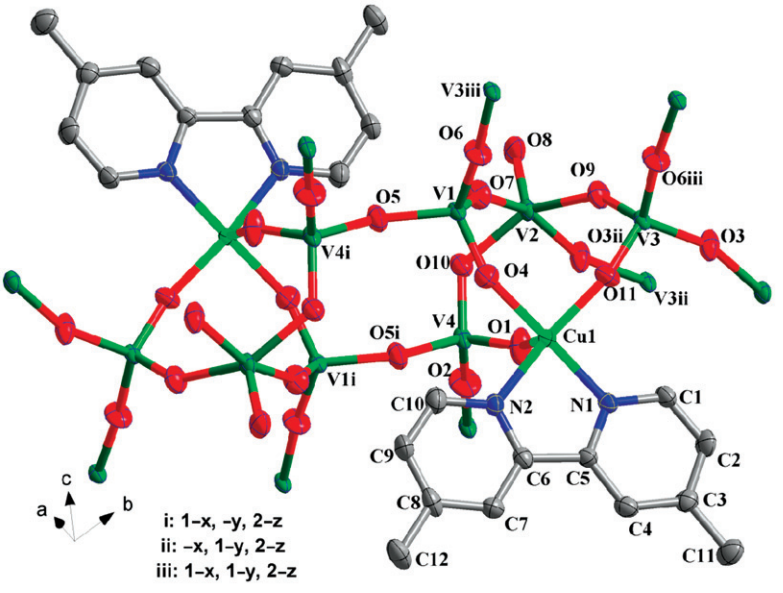

Figure 1. ORTEP drawing of **1** with thermal ellipsoids at 50% probability. All hydrogens are omitted for clarity.

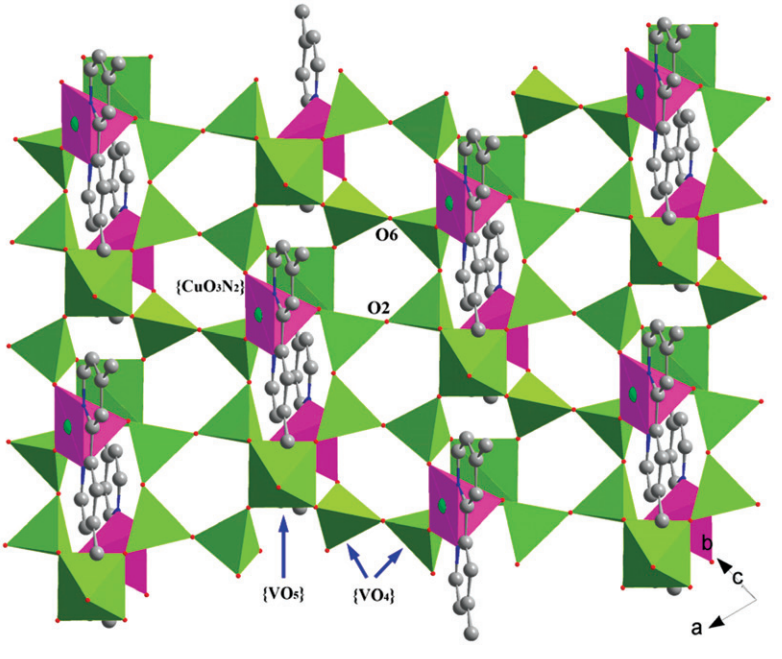

Figure 2. Polyhedral representation of the V–Cu–O layer in **1**.

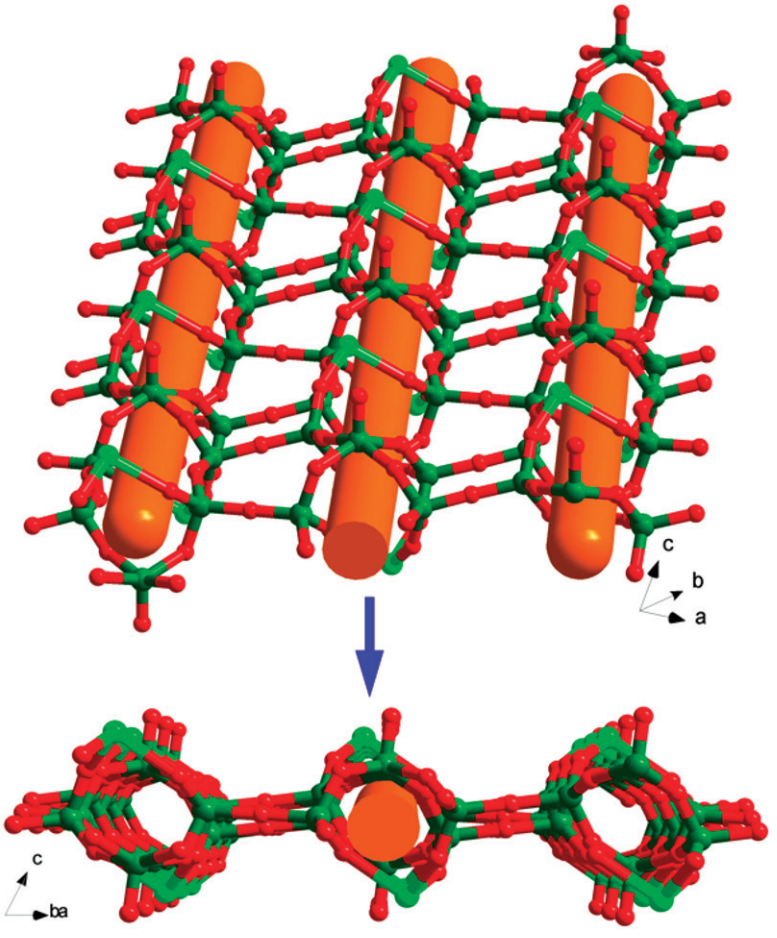

Figure 3. Two views showing the 2-D layer with tunnel structures along different directions. The tunnels are drawn as columns and all carbons, hydrogens, and nitrogens are omitted for clarity.

constructed from V–O–V(Cu) linkages (figure 3). The cylindric tunnel size is *ca* $4.2 \times 4.4\,\text{Å}^2$.

There exist extensive intermolecular interactions among $\{V_8O_{21}\}_n$ layers, including hydrogen bonding and aromatic π–π stacking, which build a 3-D supramolecular solid of **1**. As shown in figure 4, the close contact distance between adjacent aromatic rings of mbpy is 3.376–3.648 Å.

The bond valence sum (BVS) calculations [21] indicate that V(1) (5.336), V(3) (5.301), and V(4) (5.202) are in the 5+ oxidation state, while V(2) (4.456) is in the 4+ oxidation state. The BVS analysis also shows that Cu(1) (1.902) is in the 2+ oxidation state.

3.3. *Fourier transform infrared spectroscopy and TG analyses*

The IR spectrum (figure S1) of **1** shows a series of bands at 1407–1616 cm^{-1} associated with mbpy. The compound also possesses bands at 615–1004 cm^{-1} attributed

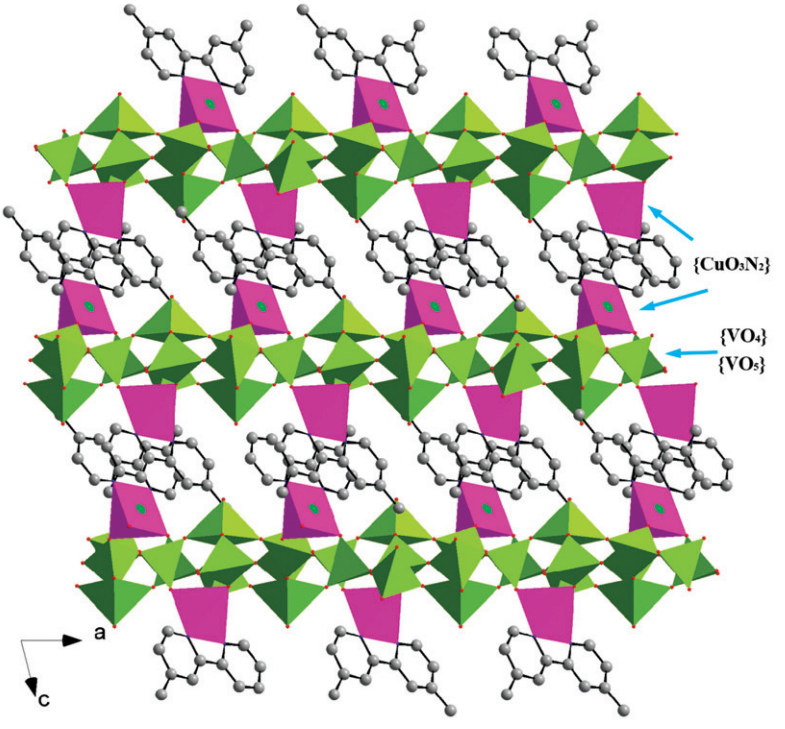

Figure 4. The packing arrangement of **1** viewed along the *b*-axis.

to ν(M=O). The broad bands in the 3135 and 3423 cm^{-1} region may be associated with intermolecular hydrogen-bonding interactions in **1** [22]. TGA of **1** (figure 5) reveals two weight losses. The first is from 280°C to 400°C with a value of 28.05% and the second is 1.01% occurring from 400°C to 460°C. This corresponds to the removal of mbpy. The whole weight loss (29.06%) is in agreement with the calculated value (28.33%).

3.4. *Voltammetric behavior of 1-CPE*

POMs are generally unstable in neutral and basic aqueous solution undergoing a series of hydrolysis processes, but is fairly stable in acidic aqueous solution. Therefore, electrochemical studies of **1**-CPE were carried out in acidic aqueous solutions.

Figure 6 presents the CV for **1**-CPE in 1 mol L^{-1} H_2SO_4 at different scan rates. In a potential range from 0.700 to 0.400 V, two pairs of redox peaks appear. The mean peak potentials $E_{1/2} = (E_{pc} + E_{pa})/2$ are 0.446 and 0.028 V (scan rate: 30 mV s^{-1}), respectively. Redox peaks should be ascribed to the redox processes of V. The CV curves of **1**-CPE redox at various scan rates were studied. When scan rate varied from 30 to 250 mV s^{-1}, peak potentials changed gradually with cathodic peak potentials shifting to negative direction and corresponding anodic peak potentials to positive direction with increasing

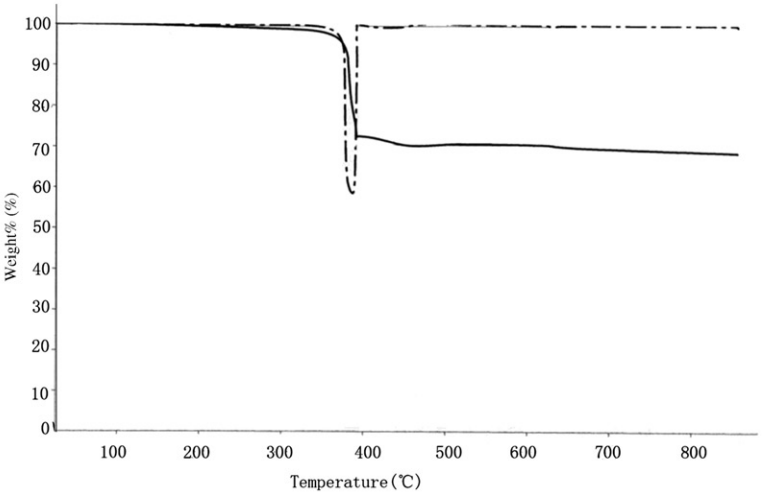

Figure 5. TG curve of **1**.

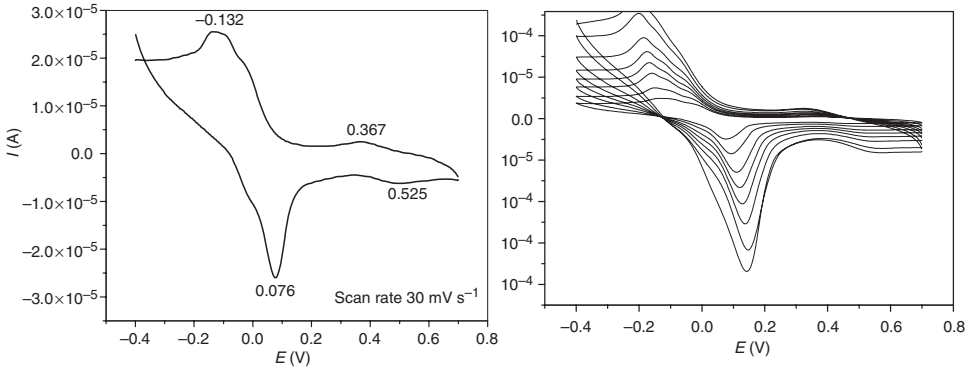

Figure 6. CV of **1**-CPE in 1 mol L^{-1} H_2SO_4 aqueous solution at different scan rates (from inner to outer: 30, 50, 80, 120, 150, 180, 200, and 250 mV s^{-1}).

scan rates. Peak currents increase with increasing scan rate. Compared with conventional POM-modified electrodes, **1**-CPE presents good stability, which is especially important for practical applications.

4. Conclusion

In this article, a new layered vanadate with tunnel structures has been prepared in which the Cu-mbpy coordinates directly to the inorganic vanadium oxide layer. The isolation of **1** further confirms that organic–inorganic hybrid vanadium oxide materials can be obtained by the introduction of different transition metal complex moieties.

Supplementary material

CCDC 756321 contains the supplementary crystallographic data for **1**. These data can be obtained free of charge *via* http://www.ccdc.cam.ac.uk/conts/retrieving.html, or from the Cambridge Crystallographic Data Centre, 12 Union Road, Cambridge CB2 1EZ, UK; Fax: +44 1223 336 033; or Email: deposit@ccdc.cam.ac.uk

Acknowledgments

This work was financially supported by the Natural Science Foundation of China (20701011), China Postdoctoral Science Foundation (20070410037 and 20801045), Doctoral Initial Foundation of Hebei Normal University (L2005B13), and the Education Department Foundation of Hebei Province (Z2006436).

References

[1] D.L. Long, E. Burkholder, L. Cronin. *Chem. Soc. Rev.*, **36**, 105 (2007).
[2] T.B. Liu, E. Diemann, H.L. Li, A.W.M. Dress, A. Müller. *Nature*, **426**, 59 (2003).
[3] C.P. Pradeep, D.L. Long, G.N. Newton, Y.F. Song, L. Cronin. *Angew. Chem. Int. Ed.*, **47**, 4388 (2008).
[4] D. Corradi, S.V. Meille, M.T. Messina, P. Metrangolo, G. Resnati. *Angew. Chem. Int. Ed.*, **39**, 1782 (2000).
[5] D.L. Long, Y.F. Song, E.F. Wilson, P. Kgerler, S.X. Guo, A.M. Bond, J.S.J. Hargreaves, L. Cronin. *Angew. Chem. Int. Ed.*, **47**, 4384 (2008).
[6] (a) Z.G. Han, Y.G. Gao, X.L. Zhai, J. Peng, A.X. Tian, Y.L. Zhao, C.W. Hu. *Cryst. Growth Des.*, **9**, 1225 (2009); (b) Z.G. Han, Y.G. Gao, C.W. Hu. *Cryst. Growth Des.*, **8**, 1261 (2008).
[7] H.Q. Tan, Y.G. Li, Z.M. Zhang, C. Qin, X.L. Wang, E.B. Wang, Z.M. Su. *J. Am. Chem. Soc.*, **129**, 10066 (2007).
[8] L.H. Bi, E.V. Chubarova, N.H. Nsouli, M.H. Dickman, U. Kortz, B. Keita, L. Nadjo. *Inorg. Chem.*, **45**, 8575 (2006).
[9] P.J. Hagrman, D. Hagrman, J. Zubieta. *Angew. Chem. Int. Ed.*, **38**, 2638 (1999).
[10] (a) H.Y. An, E.B. Wang, D.R. Xiao, Y.G. Li, Z.M. Su, L. Xu. *Angew. Chem. Int. Ed. Engl.*, **45**, 904 (2006); (b) C.M. Liu, D.Q. Zhang, D.B. Zhu. *Cryst. Growth Des.*, **6**, 524 (2006).
[11] Q.G. Zhai, X.Y. Wu, S.M. Chen, Z.G. Zhao, C.Z. Lu. *Inorg. Chem.*, **46**, 5046 (2007).
[12] (a) Z.G. Han, Y.L. Zhao, J. Peng, H.Y. Ma, Q. Liu, E.B. Wang, N.H. Hu, H.Q. Jia. *Eur. J. Inorg. Chem.*, 264 (2005); (b) Z.G. Han, T. Chai, X.L. Zhai, J.Y. Wang, C.W. Hu. *Solid State Sci.*, **11**, 1998 (2009).
[13] (a) P.J. Hagrman, J. Zubieta. *Inorg. Chem.*, **39**, 3252 (2000); (b) Y.Z. Zhou, H.P. Qiao. *Inorg. Chem. Commun.*, **10**, 1318 (2007).
[14] (a) B.E. Koene, N.J. Taylor, L.F. Nazar. *Angew. Chem. Int. Ed.*, **38**, 2888 (1999); (b) Y.G. Li, M. Yuan, E.B. Wang, R.D. Huang, C.W. Hu, N.H. Hu, H.Q. Jia. *J. Chem. Soc., Dalton Trans.*, 331 (2003).
[15] (a) D.R. Xiao, Y. Hou, E.B. Wang, Y.G. Li, J. Lü, L. Xu, C.W. Hu. *J. Mol. Struct.*, **691**, 123 (2004); (b) Y. Oka, T. Yao, N. Yamamoto. *J. Solid State Chem.*, **150**, 330 (2000); (c) P. Millet, C. Gasquères, J. Galy. *J. Solid State Chem.*, **163**, 210 (2002); (d) W.W. Li, Q. Wang, W.S. You, L.J. Qi, L.M. Dai, Y. Fang. *Inorg. Chem. Commun.*, **12**, 1185 (2009).
[16] G. Ferey. *Chem. Mater.*, **13**, 3084 (2001).
[17] S.Y. Zhang, L.J. Ci, H.R. Liu. *J. Phys. Chem. C*, **113**, 8624 (2009).
[18] G.M. Sheldrick. *SHELXL 97, Program for Crystal Structure Solution*, University of Göttingen, Göttingen, Germany (1997); (b) *Program for Crystal Structure Refinement*, University of Göttingen, Göttingen, Germany (1997).
[19] (a) A. Müller, M. Penk, R. Rohlfing, E. Krickemeyer, J. Döring. *Angew. Chem. Int. Ed. Engl.*, **29**, 926 (1990); (b) A. Müller, F. Peters, M.T. Pope, D. Gatteschi. *Chem. Rev.*, **98**, 239 (1998); (c) Y. Xu, L.-B. Nie, D. Zhu, Y. Song, G.-P. Zhou, W.-S. You. *Cryst. Growth Des.*, **7**, 925 (2007); (d) C.J. Calzado, J.M. Clemente-Juan, E. Coronado, A. Gaita-Arino, N. Suaud. *Inorg. Chem.*, **47**, 5889 (2008);

(f) S.T. Zheng, J. Zhang, B. Li, G.Y. Yang. *Dalton Trans*., 5584 (2008); (g) B.X. Dong, J. Peng, C.J. Gomez-Garcia, S. Benmansour, H.Q. Jia, N.H. Hu. *Inorg. Chem*., **46**, 5933 (2007); (h) A. Wutkowski, C. Nather, P. Kogerler, W. Bensch. *Inorg. Chem*., **47**, 1916 (2008).
[20] S.Y. Shi, Y. Chen, B. Liu, Y.K. Lu, J.N. Xu, X.B. Cui, J.Q. Xu. *J. Coord. Chem*., **62**, 2937 (2009).
[21] I.D. Brown, D. Altermatt. *Acta Crystallogr. B*, **41**, 244 (1985).
[22] (a) V. Shivaiah, S.K. Das. *Inorg. Chem*., **44**, 7313 (2005); (b) *The Sadtler Handbook of Infrared Spectra*, Bio-Rad Laboratories, Inc., Informatics Division, Hercules, CA (2004).